中國造船暨輪機工程學刊第三十七卷第三期 民國一〇七年八月
Journal of Taiwan Society of Naval Architects and Marine Engineers, Vol.37, No.3, pp.127-136, 2018

INVESTIGATION OF THE SEAKEEPING PERFORMANCE OF TWIN HULL VESSELS BY DIFFERENT COMPUTATIONAL METHODS

C.-T. Lin[*1] T.-Y. Lin[*] Y.-W. Hsieh[**] L. Lu[**] C.-Y. Hsin[**] C.-W. Lin[*,]**

[*]CR Classification Society
[**]Department of Systems Engineering and Naval Architecture, National Taiwan Ocean University

Keywords: Catamaran, Panel Method, RANS, Seakeeping Performance

ABSTRACT

The seakeeping performances of wave piercing high speed catamaran (CAT-I) was computed and analyzed by different computational methods in this paper. The purpose is to investigate the hydrodynamic characteristics of twin hull vessels for installing the motion suppressing devices such as RCS (riding control system). The potential flow method and viscous flow RANS (Reynolds Averaged Navier-Stokes) method were used for computations. The comparisons of results from different computational methods serve two objectives. The first one is for the verification purpose to ensure the accuracy of computations. Secondly, by comparing results with experimental data, the results not only show the numerical errors, but also reveal the different features of each method. For example, the viscous and nonlinear effects of forces and flow field can thus be identified. From the preliminary results, the comparisons between numerical predictions and experimental data show a good agreement for seakeeping performances, as well as some differences near the resonance frequencies. Overall, the viscous flow RANS method demonstrates better predictions in seakeeping based on the verification and validation analysis.

INTRODUCTION

With the vigorous development of commercial activities, the choice and design of regional maritime transport is becoming more and more important. High-speed passenger ships have become one of the most important transport for maritime traffic in order to meet the requirements of safety and passenger comfort during navigation and the trend of high speed modern ships. For ship design, the catamaran has a large area of the work deck for transport purposes; Compared to a monohull with the same displacement, the catamaran has a larger transverse stability to increase navigation comfort, and high-speed planing type catamaran has smaller resistance in high speed to reduce the cost of navigation. The combination of these advantages is especially of interest to transportation of lightweight cargo, in particular when high service speeds can be maintained. The catamaran is often used in high speed military boats, ferry or yacht and other passenger ships.

In the past, most catamaran vessels were designed as ferry vessels and operate in protected or restricted environments. But with economies of scale, catamarans were designed with the increasing length and forward speed to operate in a far more demanding open-sea environment. Moving away from the protected coastal area, the seakeeping properties of catamarans become more and more important [1]. Compared to mono-hull ships of the same tonnage, twin-hull vessels have larger space and the slender hull makes the resistance relatively small. However, when the sea is rough, the pitch and roll motion of the hull may easily cause discomfort to the passengers, which limits the advantage that the catamaran can have high

[1] Corresponding author (ctlin@crclass.org)

stability only in calm sea. To improve the seakeeping capability of the catamaran in heavy waves, the concept of wave-piercing catamaran was conceived in 1983. The wave-piercing catamaran configuration consists of a centre bow, which provide reserve buoyancy in heavy waves, and two slender side hulls. The centre bow hull is connected with two side hulls by means of a cross structure, which offer useful deck area. This complex hull form shows outstanding seakeeping capability in waves [2].

About the literature of the past, model test method, potential flow method and viscous flow RANS method are the main tools to investigate the catamaran motion in waves. In the past, subject to the computational capability of computers, the model testing was relatively accurate and reliable, but the increasing development of computational techniques and numerical approach has made the potential theory method and CFD method possible to study on this issue. Comparing with model test may take a long period and need relatively high cost, potential theory method and CFD method are more efficient at a lower cost. On the other hand, CFD method can be effective to take into account for the viscous and all nonlinear effects such as the wave broken, green water on deck and water entry of cross structure sufficiently.

This paper discusses CFD results for a wave piercing high-speed catamaran (CAT-I) [3] advancing in regular waves, and includes a rigorous verification and validation (V&V) study, prediction of seakeeping performances, and comparison with model experimental data. Simulations were performed with two different computational methods, potential flow method and viscous flow RANS method, to ensure the accuracy of computation and the different features of each method.

COMPUTATIONAL METHODS

The early applications of computational fluid dynamics (CFD) to seakeeping problems involved solution techniques based on the assumptions of potential flows coupled with small amplitude motions. In 1957, Korvin-Kroukovsky and Jacobs [4] established a theory which made use of two dimensional derived numerical results of oscillating sections to assess the three dimensional overall ship hydrodynamic mass and damping coefficients for pitch and heave motion in head waves. This method, called the ordinary strip theory, is a zero speed potential slender-body theory in which the forward speed effect is included using a simple approximation. To simulate more complex motions of ship, Salvesen *et al*. [5] introduced a new strip theory that could predict heave, pitch, sway, roll and yaw, assuming potential flows, linear and harmonic oscillatory motions and ship lateral symmetry. In many problems, the two dimensional effects dominate the flow and it is the reason why the strip theory can predict the ship motions and loads with reasonable accuracy. However, when three-dimensional effects are prominent, for example, in the flow behavior between the two hulls of a catamaran, it can be expected that the strip theory fails to predict the motions accurately. On the other hand, poor accuracy was reached in further strip theory based computations for horizontal plane motions, particularly for roll motion, due to its viscous nature. Faltinsen and Zhao [6] also stated that the strip theory was questionable when applied at high speeds, since it accounts for the forward speed in a simplistic manner. Discrepancies between the strip theory and experiments for higher speed vessels, or highly non-wall sided hull forms, have therefore motivated research to develop more advanced theories, such as the 3-D Rankine panel method and unsteady RANS methods. At present, CFD simulations have been also performed for more complex ship geometries. Castiglione *et al*. [7] simulated the seakeeping characteristics of the DELFT 372 catamaran in incoming regular head waves by RANS code. Comparison with the strip theory solutions shows that the RANS method predicts ship motions with higher accuracy and allows the detection of nonlinear effects. Bouscasse *et al*. [8] have conducted the experimental study on seakeeping performance of high-speed catamaran in head waves, analyzed the influence of ship speed and wavelength on added resistance, and simulated the ship motions in irregular waves. Tezdogan *et al*. [9] performed a fully nonlinear unsteady RANS simulation to predict the ship motions and added resistance of a full scale KRISO Container Ship model by using a commercial RANS solver. The results are validated against available experimental data and are found to be in good agreement with the experiments.

1. Numerical Method

The commercial CFD software "HydroStar," which was developed by Bureau Veritas, is based on the potential flow theory to solve the problem under the frequency domain and the assumption for small amplitude theory, and uses the three-dimensional panel method to discretize the model. Since the potential flow theory does not consider the viscous effect of the fluid, the software uses the artificial correction method to correct the viscous effect, especially the roll damping.

In STAR-CCM+, Navier-Stokes equations is solved to model the fluid flow around the ship body. There are a range of options provided by the STAR-CCM+ software package for solving the Navier-Stokes equations. These include Reynolds averaging (with a number of options for closure of the turbulent stress terms), large eddy simulation (LES), detached eddy simulation (DES), and inviscid potential flow. The work presented here utilizes the Reynolds averaged Navier Stokes equations approach (RANS). The mean mass and momentum transport equation can be written as follows

$$\frac{\partial \rho}{\partial t} + \nabla \cdot \left[\rho(\bar{\mathbf{v}} - \mathbf{v}_g) \right] = 0 \tag{1}$$

$$\frac{\partial}{\partial t}\left(\rho \bar{\mathbf{v}}\right) + \nabla \cdot \left[\rho \bar{\mathbf{v}} (\bar{\mathbf{v}} - \mathbf{v}_g) \right] = -\nabla \cdot \bar{p}\mathbf{I} + \nabla \cdot \left(\mathbf{T} - \rho \overline{\mathbf{v}'\mathbf{v}'} \right) + \mathbf{f}_b \tag{2}$$

where ρ is the density, $\bar{\mathbf{v}}$ and $\bar{p}$ are the mean velocity and pressure, respectively, $\mathbf{v}_g$ is the reference frame velocity relative to the laboratory frame, $\mathbf{I}$ is the identity tensor, $\mathbf{T}$ is the stress tensor, and $\mathbf{f}_b$ is the resultant of the body forces (such as gravity and centrifugal forces).

2. Ship Geometry and Model Test

A full scale model of the CAT-I (Fig. 1) catamaran models were used within this study. The main geometric characteristics of CAT-I catamarans are summarized in Table 1. Experiments with the CAT-I catamaran model were carried out in SSPA's Maritime Dynamic Laboratory. During the model tests, the response amplitude operators (RAO) of the ship model for surge, sway, heave, pitch, roll and yaw motion related to the wave elevation at the center of gravity section were measured. The experimental data include the RAO of heave and pitch motion for CAT-I catamaran model advancing in regular head waves, at wave frequencies ranging from ω = 0.5-1.3 (rad/s). Fig. 2 shows some of the selected motion responses of the CAT-I at a nominal speed of 30 knots (Fn = 0.77) in regular head waves.

3. Physics Modelling

Within the RANS solution approach to the Navier-Stokes equations, STAR-CCM+ offers a wide variety of turbulence modelling options. The turbulence model selected in this study was a realizable k-ε two-layer model, which is extensively used for industrial applications and provide a good compromise between robustness, computational cost and accuracy. The volume of fluid (VOF) method was used to model and position the free surface, either with a flat or regular wave. The VOF model uses the assumption that the same basic governing equations as those used for a single phase problem can be solved for all the fluid phases

Table 1 Principal particulars of the CAT-I.

CAT-I	
LBP (m)	40.50
Beam overall, B (m)	12.50
Beam of each hull at LWL (m)	3.40
Draught, D(m)	1.50
Hull spacing between hull centre-line (m)	9.10
Displacement (tonnes)	223.00
VCG (m)	4.05
LCG aft of F.P. (m)	24.01
Radius of gyration K_{xx} (m)	4.37
Radius of gyration K_{yy} (m)	11.32
Radius of gyration K_{zz} (m)	11.89

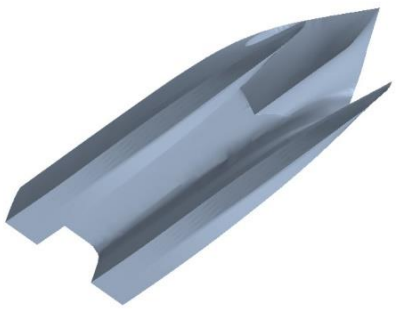

Fig. 1 Configuration of the wave-piercing catamaran (CAT-I)

present within the domain, as it is assumed that they have the same velocity, pressure and temperature. This means that the equations are solved for an equivalent fluid whose properties represent the different phases and their respective volume fractions. In this study, a second-order convection scheme was used throughout all simulations in order to accurately capture sharp interfaces between the phases. Fig. 3 demonstrates how the free surface was represented in STAR-CCM+ by displaying the water volume fraction profile on the hull. In the figure, a value of 0.5 for the volume fraction of water implies that a computational cell is filled with 50% air. This value therefore indicates the position of the water-air interface, which corresponds to the free surface.

In order to simulate realistic ship behavior, a dynamic fluid body interaction (DFBI) model was used with the ship free to move in the pitch and heave directions for STAR-CCM+. The DFBI model enabled the RANS solver to calculate the exciting force and moments acting on the ship hull due to waves, and to solve the governing equations of rigid body motion in order to re-position the rigid body.

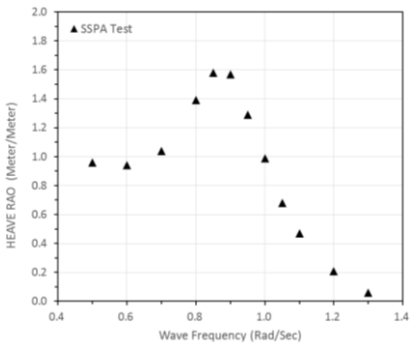

(a) Heave RAO.

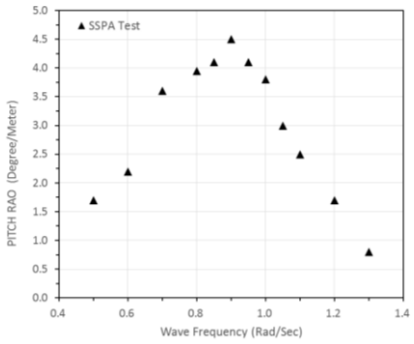

(a) Pitch RAO.

Fig. 2 Motion response of the CAT-I at 30 knots (head wave).

4. Choice of the Time Step

The Courant number (*CFL*), which is the ratio of the physical time step (Δt) to the mesh convection time scale, relates the mesh cell dimension (Δx) to the mesh flow speed (U_0) as given by

$$CFL = \frac{U_0 \cdot \Delta t}{\Delta x} \tag{3}$$

The Courant number is typically calculated for each cell and should be less than or equal to 1 for numerical stability. In STAR-CCM+, for the prediction of ship responses to incident regular waves, the *CFL* of free surface set below 0.5 to best capture VOF waves.

COMPUTATIONAL DOMAIN AND BOUNDARY CONDITIONS

In STAR-CCM+ computational domains for a seakeeping analysis in waves, an overset mesh was used to facilitate the motions of the full-scale CAT-I catamaran model. Compared to the overset mesh approach, which moves with the hull over a static background mesh of the whole domain, Rigid and deforming mesh motion methods have distinct disadvantages when simulating bodies with large amplitude motions. The rigid motion approach causes difficulties for free surface refinement, especially in pitch, and deforming meshes may lead to cell quality problems. For this reason, using the overset mesh approach saves computational costs, and allows the generation of a sufficiently refined mesh configuration around the free surface and the ship hull, without compromising the solution's accuracy. Without the use of the overset mesh, simulating a full-scale ship model in waves would require a very high cell number, requiring much more

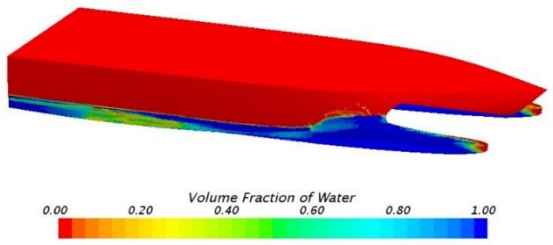

Fig. 3 Free surface representation on the ship hull.

computational power.

When using the overset mesh feature, two different regions were created to simulate ship responses in waves, namely background and overset regions. A general view of the computation domain with the Catamaran hull model and the notations of selected boundary conditions are depicted in Fig. 4. It illustrates that a velocity inlet boundary condition was set in the negative *x*-direction, where incident regular waves were generated. The positive *x*-direction was modelled as a pressure outlet. The top and bottom boundaries were both selected as pressure outlet. The symmetry plane, as the name suggests, has a symmetry condition, and the side of the domain (positive *y*-direction) has a symmetry plane boundary condition as well. The top, bottom and side boundaries could have been set as a slip-wall or symmetry plane. The selection of boundary conditions from any appropriate combination would not affect the flow results significantly, provided that they are placed far enough away from the ship hull, such that the flow is not disturbed by the presence of the body. Also, the pressure outlet boundary condition was set behind the ship since it prevents backflow from occurring and fixes static pressure at the outlet.

5. Wave Conditions

As stated previously, by using "HydroStar", the numerical simulations of CAT-I advancing in regular head waves were performed at a nominal speed of 30 knots and wave frequency ranging from ω = 0.5-1.3 (rad/s). And for "STAR-CCM+," the numerical simulations of CAT-I were performed at a nominal speed of 30 knots and four difference wave frequency conditions, respectively 0.6, 0.8, 0.9, and 1.0 (rad/s), due to computational costs. The first order VOF wave model with a first order approximation to the Stokes theory of waves is adopted with wave height fixed at 1.0 m. The VOF Wave model generates a number of field functions that are based on the wave parameters. These field functions can be used as boundary and initial conditions in appropriate nodes on the object tree. The first order wave mentioned here is the wave that generates regular periodic sinusoidal profile. It is also of note that the analyses were performed using deep water conditions.

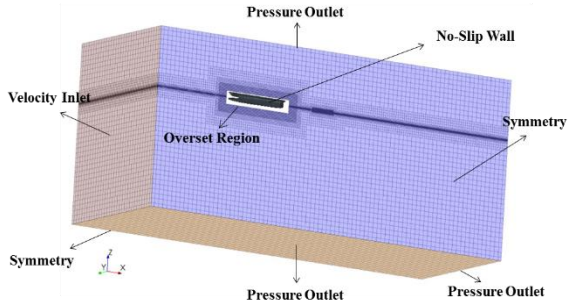

Fig. 4 A general view of the background and overset regions and the applied boundary conditions.

6. Mesh Generation

Mesh generation was performed using the automatic meshing facility in STAR-CCM+, which uses the Cartesian cut-cell method. A trimmed cell mesher was employed to produce a high-quality grid for complex mesh generating problems. The computation mesh had areas of progressively refined mesh size in the area immediately around the ship hull, as well as the expected free surface and in the wake that was produced by the ship, to ensure that the complex flow features were appropriately captured. The refined mesh density in these zones was achieved using volumetric controls applied to these areas. The mesh was structured, rigid and body-fixed, so that motions of the body corresponded to the movement of grid points. The most refined mesh areas around the hull remained within the boundaries of the overset domain. When generating the volume mesh, extra care was given to the overlapping zone between the background and overset regions. To simulate ship motions in waves, the mesh was generated based on the guidelines for ship CFD applications from ITTC [10]. According to these recommendations, a minimum of 80 cells per wavelength should be used on the free surface. Additionally, a minimum of 20 cells was used in the vertical direction where the free surface was expected. Figure 5 shows a cross-section of the computation mesh. The overset mesh region around the ship hull is also noticeable in Fig. 5. Fig. 6 shows the surface mesh on the CAT-I hull.

VALIDATION AND VERIFICATION

To quantify errors and uncertainties in CFD sim-

ulations by STAR-CCM+, verification and validation (V&V) was performed following the approach methodology [11] for convergence study. Numerical errors and uncertainties are due to the numerical solution of the mathematical equations and include discretization errors, computer round-off errors, artificial dissipation and incomplete iterative and grid convergence. Verification procedure provides an estimation of the numerical errors, given by the sum of the iterative errors and of grid and time-step spacing errors. A minimum of three solutions is required to evaluate convergence with respect to the input parameters, so that the solutions changes for medium-fine, $\varepsilon_{21} = S_2 - S_1$, and coarse-medium, $\varepsilon_{32} = S_3 - S_2$, solutions are computed. By the evaluation of their ratio, $R = \varepsilon_{21} / \varepsilon_{32}$, the following convergence conditions are possible: (1) Monotonic convergence ($0 < R < 1$); (2) Oscillatory convergence ($R < 0$); and (3) divergence ($R > 1$).

For monotonic convergence (1), the order of accuracy, p_{RE}, and the error, δ_{RE}, are computed using the Richardson extrapolation (RE) method. For numerical uncertainties, several methods can be used, including the correction factor (CF) method and the factor of safety (FS) method. Within the last method, a better distance metric, P, to the asymptotic range is used instead of the correction factor and is defined as the ratio of p_{RE} to p_{th}.

$$P = \frac{p_{RE}}{p_{th}} \tag{4}$$

When the solutions are in the asymptotic range, then $p_{RE} = p_{th}$.

However, in many circumstances, solutions are far from the asymptotic range such that p_{RE} is greater or smaller than p_{th}. One of the improvements of the FS method, with respect to the CF method, is that it overcomes the too small uncertainty estimates for $p_{RE} > p_{th}$. Furthermore, it achieves and overall 95% confidence interval for the estimated uncertainty to bound the true error. The FS method uncertainty, U_{FS}, is given by

$$\begin{aligned} U_{FS} &= FS(P)\left|\delta_{RE}\right| \\ &= \begin{cases} (2.45 - 0.85P)\left|\delta_{RE}\right|, & 0 < P \le 1 \\ (16.4P - 14.8)\left|\delta_{RE}\right|, & P > 1 \end{cases} \end{aligned} \tag{5}$$

The numerical uncertainty, U_{SN}, is composed of the iterative, U_I, grid, U_G, and time-step, U_T, uncertainties

$$U_{SN}^2 = U_I^2 + U_G^2 + U_T^2 \tag{6}$$

Modeling errors are due to the assumptions and approximations in the mathematical representations of the physical problem, which include geometry, boundary conditions, mathematical governing equations and turbulence models. Validation procedure gives an estimation of the modeling errors, δ_{SMA}, and uncertainties, by using benchmark experimental data. The validation uncertainty, U_V, is computed as

$$U_V^2 = U_D^2 + U_{SN}^2 \tag{7}$$

where U_D is the uncertainty of the experimental data.

The comparison error, E, is defined as the difference between the experimental data, D, and the simulation results, S

$$E = D - S \tag{8}$$

When $|E|$ is within the $\pm U_V$ interval, the solution is validated at the U_V level, otherwise the sign and magnitude of E are used to estimate the error deriving from the modeling assumptions.

The near-resonant physical conditions for heave motions were selected for V&V study (Fn = 0.77, ω =

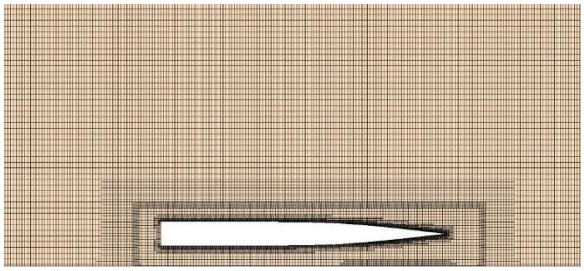

Fig. 5 A cross-section of the computation mesh.

Fig. 6 Surface mesh on the hull.

Table 2 Grids

	Coarse	Medium	Fine
Overset	198,054	458,161	774,105
Background	297,090	754,067	1,702,507
Total	495,144	1,212,228	2,476,612

0.9 rad/s, wave height = 0.5 m), as the large ship motions, expected in this condition, make this the worst-case test. The verification parameters are the RAO of heave and pitch motions, A_3 and A_5, respectively.

1. Verification Studies

A systematic time step converge study was carried out with a time step refinement ratio of $\gamma_T = \sqrt{2}$ on the finest grid, while a grid convergence study was conducted on the medium time step. In order to verify the mesh-independence of the solution, medium and coarse mesh were generated by coarsening the finer grid by $1/\sqrt{2}$ in each direction with a tri-linear interpolation algorithm, so that the grid distribution and shape could be as close as possible to the original shape. The resulting coarse, medium and fine grid sizes are 0.5, 1.2 and 2.5 million, respectively (Table 2). Iterative convergence was assessed, in that the residuals of each flow variable drop four orders of magnitude after 5 iterations per time step. Furthermore, U_I values for each variable range within 0.05(% of S_1) < U_I < 0.2(% of S_1), so that they are negligible in comparison to the grid and time-step errors.

Results for grid and time step convergence studies are summarized in Table 3. Monotonic convergence was achieved ($0 < R_G < 1$) for A_3 and A_5; therefore the generalized Richardson extrapolation (RE) was used in estimating the grid order of accuracy, P_G, and the grid error δ_G. The FS method was used to compute the numerical errors and uncertainties, U_G. Results show that P_G ranges within 0.25 < P_G < 0.5, indicating that the solutions are far from the asymptotic range ($P_G = 1$). The same approach was applied for the time step convergence study. The monotonic convergence between solutions was assessed ($0 < R_T < 1$). Results show that the solutions are closer to the asymptotic range for all the variables ($0.9 < P_T < 1.1$). By a comparison between grid and time step studies, U_G values are higher than U_T, which is relatively small. Therefore, grid errors are the significant source of numerical uncertainty. Overall, verification results can be considered satisfactory for RAO of ship motions, as the numerical convergence was achieve.

2. Validation Studies

To determine modeling errors, the numerical results were compared to the experimental data. As the uncertainty in experimental data is not given, fairly low value of $U_D = 2.5\%$ of the data was assumed. The validation uncertainty, U_V, and the comparison error, E, defined as the difference between data and the numerical value of the finer simulation ($E = D - S_1$) were calculated for A_3 and A_5. The values are summarized in Table 4. For RAO of heave motion, A_3, in fact, the comparison error, E, is less than the validation uncertainty, U_V, hence it is validated at the U_V level of 9.5% of *D*. RAO of the pitch motion, A_5, is also validated at the U_V level of 10.4% of *D*.

Results indicate that improvements are still necessary for computations involving unsteady problems. Nonetheless, the validation results can be considered encouraging for such a complicated calculation and are reasonable if compared to the report by Castiglione *et al.* [7].

RESULTS AND DISCUSSION

This section will outline the simulation results achieved during this study, and will also provide some comparison with experimental results and the results from potential flow theory. It will then present a discussion on the observation of the results.

Fig.7 shows the numerical results of heave and pitch motions as a function of wave frequency, ω.

Table 3 Verification of RAO of heave and pitch motions

	R_G	$(p_{RE})_G$	P_G	U_G (% of S_1)	R_T	$(p_{RE})_T$	P_T	U_T (% of S_1)
A_3	0.71	0.99	0.49	9.95%	0.50	2.00	1.00	3.79%

A_5	0.84	0.51	0.25	9.75%	0.48	2.14	1.07	2.38%

RAOs are computed both by HydroStar and STAR-CCM+. The RAO of heave and pitch motions are defined, respectively, as

$$A_3 = \frac{x_3}{a} \tag{9}$$

$$A_5 = \frac{x_5}{a} \tag{10}$$

where a is the wave amplitude and x_3 and x_5 are the heave and pitch motion response in regular head waves. Heave and pitch motions are referred to the center of gravity of the ship.

For HydroStar, there is a good correlation between numerical and experimental results except the one around the resonance region of pitch motions. The experimental measurements are lower than numerical predictions. This may be due to the three-dimensional panel method cannot consider the nonlinear effects and the ship geometry above the water line. For

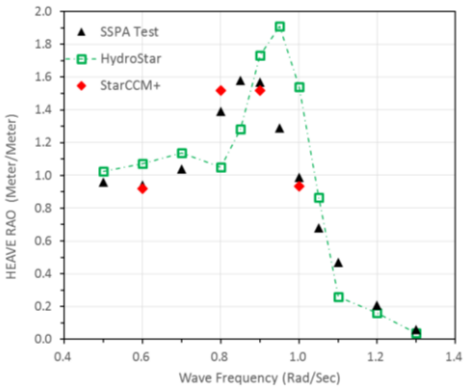

(a) Heave RAO.

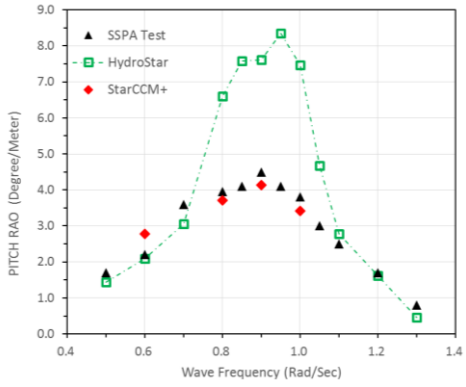

(b) Pitch RAO.

Fig. 7 Motion response of the CAT-I at 30 knots (head wave).

STAR-CCM+, there is satisfactory agreement among all results. The comparison between numerical and experimental results shows a good agreement.

CONCLUSIONS

This paper discusses CFD results for wave piercing high speed catamaran (CAT-I) advancing in regular head waves, and includes a rigorous verification and validation study, comparison with available experimental data. The seakeeping performances of CAT-I was computed and analyzed by potential flow method and viscous flow RANS method.

To quantify errors and uncertainties in CFD simulations by STAR-CCM+, verification and validation (V&V) was performed following the approach methodology for convergence study. For RAO of heave motion, the comparison error is less than the validation uncertainty, hence it is validated at the U_V level of 9.5% of D. RAO of pitch motion is also validated at the U_V level of 10.4% of D. Results indicate that improvements are still necessary for computations involving unsteady problems. For the CFD simulation, the potential flow methods and viscous flow RANS method are applied to predict the seakeeping characteristics of CAT-I in regular head waves by using the commercial CFD software “HydroStar” and “STAR-CCM+”, respectively. For HydroStar, there is a good correlation between numerical and experimental results except the one around the resonance region of pitch motions. The experimental measurements are lower than numerical predictions. For STAR-CCM+, there is satisfactory agreement among all results. The comparison between numerical and experimental results shows a good agreement.

Overall, the viscous flow RANS method demonstrates better predictions in seakeeping of head sea based on the verification and validation analysis. This may be due to the face that three-dimensional panel potential flow method cannot consider the nonlinear effects and the ship geometry above the water line. If the hull geometry is too complicated or the ship motion is too large, it will lead to errors. In addition, the

other four degrees of freedom cannot be discussed due to insufficient calculation results. This report will be further explored in the future.

REFERENCES

1. Van't Veer, A.P., "Behavior of Catamarans in Waves," Ph.D. Thesis, Faculty of Design, Engineering and Production, Delft University of Technology, Delft, Netherlands (1998).
2. Soars, A.J., *The Hydrodynamic Development of Large Wave-piercing Catamarans*, Advanced Multihull Designs Pty Ltd (1993).
3. Fang, C.-C. Fang and H.-S. Chan, "Investigation of seakeeping characteristics of high-speed catamaran in waves," *J. Mar. Sci. Technol.*, Vol. 12, pp. 7-15 (2004).
4. Korvin-Kroukovsky, B.V. and W.R. Jacobs, "Pitching and heaving motions of a ship in regular waves," *Trans. SNAME*, Vol. 65, pp. 590-692 (1957).
5. Salvesen, N., E.O. Tuck, and O. Faltinsen, "Ship motions and sea loads," *Trans. SNAME*, Vol. 78, pp. 250-287 (1970).
6. Faltinsen, O. and R. Zhao, "Numerical prediction of ship motions at high forward speed," *Philos. Trans. Phys. Sci. Eng.*, Vol. 334, pp. 241-257 (1991).
7. Castiglione, T., F. Stern, S. Bova, and M. Kandasamy, "Numerical investigation of the seakeeping behavior of a catamaran advancing in regular head waves," *Ocean Eng.*, Vol. 38, pp. 1806-1822 (2011).
8. Bouscasse, B., R. Broglia and F. Stern, "Experimental investigation of a fast catamaran in head waves," *Ocean Eng.*, Vol. 72, pp. 318-330 (2013).
9. Tezdogan, T., T.K. Demirel, P. Kellett, K. Khorasanchi, A. Incecik, and O. Turan, "Full-scale unsteady RANS CFD simulations of ship behaviour and performance in head seas due to slow steaming," *Ocean Eng.*, Vol. 97, pp. 186-206 (2015).
10. International Towing Tank Conference (ITTC), "Practical guidelines for ship CFD applications," *Proc. 26th Conf. ITTC*, Rio de Janeiro, Brazil (2011).
11. Xing, T. and F. Stern, "Factors of safety for Richardson extrapolation," *J. Fluids Eng.*, Vol. 132, 061403 (2010).

NOMENCLATURE

a	wave amplitude
A_3	heave RAO
A_5	pitch RAO
CFD	computational fluid dynamics
CFL	Courant number
D	experimental data
DFBI	dynamic fluid body interaction
E	comparison error
EFD	experimental fluid dynamics
FS	factor of safety
Fn	Froude number
$\mathbf{f}$	resultant force acting on the ship
$\mathbf{f}_b$	resultant of the body forces
$\mathbf{I}$	identity tensor
m	mass of the ship
$\bar{p}$	mean pressure
p_{th}	theoretical order of accuracy
p_{RE}	estimated order of accuracy by RE method
P	distance metric to the asymptotic range
ρ	density
R	ratio between solution changes
RANS	Reynolds averaged Navier-Stokes
RAO	response amplitude operator
RCS	riding control system
RE	Richardson extrapolation
SWATH	small water-plane area twin hull ship
S_i	numerical solution
$\mathbf{T}$	stress tensor
t	time
U_0	flow speed
U_{FS}	FS method uncertainty
U_I	iterative uncertainty
U_G	grid uncertainty
U_T	time-up uncertainty
U_{SN}	simulation numerical uncertainty
U_V	validation uncertainty
U_D	experimental data uncertainty
VOF	volume of fluid
V&V	verification and validation
$\mathbf{v}$	velocity of the center of mass
$\bar{\mathbf{v}}$	mean velocity
$\mathbf{v}_g$	reference frame velocity relative to the laboratory frame mean velocity
ω	wave frequency
x_3	heave motion response
x_5	pitch motion response
ε_{ij}	change between solutions i and j
γ_T	refinement ratio

δ_{RE}	error estimate by RE method	Δx	mesh cell dimension
δ_{SMA}	error estimate from the modeling assumptions		
Δt	physical time step		

以不同計算方法研究雙體船的耐波性能

林均達 * *林宗岳* * *謝侑雯* ** *呂玲* ** *辛敬業* * *林正文* *,***

*財團法人中國驗船中心
**國立臺灣海洋大學　系統工程暨造船學系

關鍵詞：雙體船，小板法，RANS，耐海性能模擬

摘　　要

本文採用不同的計算方法進行計算並分析穿浪型高速雙體船的耐波性能，其目的是研究雙體船的水動力特性。計算上採用勢流方法和 RANS 方法並進行結果比較。比較不同方法的計算結果有兩個目標。第一個是用於驗證目的，並確保計算的準確性；其次，通過計算結果與實驗數據的比較，不僅顯示了數值的誤差，且揭示了每種方法的不同特徵。從基於驗證及確認分析的結果來看，其證明了 RANS 方法在耐波性方面有著更好的預測能力。

(Manuscript received Oct. 07, 2018,
Accepted for publication Jan. 09, 2019)